IBSBI 2011, October 13-15, 2011, Athens, Greece

GENERALISED FRAGILITY CURVES FOR STRAIGHT BRIDGES, FOR ARBITRARY ANGLE OF INCIDENCE OF THE SEISMIC ACTION, INCLUDING SOIL-BRIDGE INTERACTION

Ioannis Moschonas[1], Andreas Kappos[2] and Anastasios Sextos[3]

[1,2,3] Aristotle University of Thessaloniki, Dept. of Civil Engineering, Greece
e-mail: imoschon@civil.auth.gr, ajkap@civil.auth.gr, asextos@civil.auth.gr

ABSTRACT: An analytical procedure is presented for the derivation of generalised seismic fragility curves for bridges subjected to seismic action with any angle of incidence, based on an extended version of static nonlinear analysis. The procedure is applied to a straight bridge taking also into account soil-bridge interaction, to assess its effect on bridge response and fragility.

KEY WORDS: BRIDGES; ANGLE OF INCIDENCE; FRAGILITY; SOIL-BRIDGE INTERACTION; VULNERABILITY.

1 INTRODUCTION

The effect of the angle of incidence of the incoming seismic waves on the fragility of bridges was investigated by the authors [8, 9]; to this purpose the static nonlinear analysis procedure was extended to account for the angle of incidence effect and a previously proposed analytical methodology for the derivation of fragility curves in the principal bridge directions [10] was also adopted to this general case. The new procedure was then applied to both a straight bridge [8] and a skew bridge [9].

A crucial parameter that affects bridge response is the dynamic interaction between the bridge and the supporting ground, in particular at the abutment-backfill-embankment interface, subsequent to the closure of the longitudinal gap between the deck and the abutment backwall. In previous works soil-bridge interaction effects for seismic action acting along the principal bridge directions was investigated both with regard to bridge response [5-7] and bridge fragility [10]. The effect of the angle of incidence was also investigated, but only for the response of a curved bridge using dynamic analysis [15]. Hence, a next step is the investigation of soil-bridge interaction effects on bridge response using *static* nonlinear analysis, extended for the case of arbitrary angle of incidence of the seismic action, and the derivation of fragility curves for this general case, which is the subject of the present work.

2 METHODOLOGY FOR THE DERIVATION OF FRAGILITY CURVES

The proposed methodology for the derivation of both pushover and fragility curves for arbitrary angle of incidence of the seismic action is summarized below; a more detailed description can be found elsewhere [9].

At first, the earthquake motion is analysed into its principal components [2, 11]. The principal components with the maximum and the intermediate intensity are horizontal (major and minor horizontal component, respectively) and in the general case they are considered as acting simultaneously (dual-component seismic action). In the simpler case, only the major horizontal component is taken into account (single-component seismic action). Principal horizontal components are then used to derive the horizontal earthquake components E_x and E_y acting along the longitudinal and the transverse bridge direction, respectively, which are then used at the next step described below.

The next step is the derivation of pushover curves for various angles of incidence for single or dual component seismic action applying the proposed methodology, which is based on the combination of responses along the principal bridge directions. The interaction between biaxial moment and axial force at critical pier sections or biaxial shear force and axial force at bearings (wherever present) is also taken into account.

During the following step, damage states are defined firstly in a qualitative manner, e.g. using definitions provided in HAZUS [4], and then they are quantified using bridge deck displacements, separately for damage developed at the bridge and the abutment-backfill-foundation (ABF) system. Regarding the former type of damage, bridges are first classified into three categories according to their seismic energy dissipation mechanism, and then damage states are defined directly on the corresponding bilinearised 'typical' bridge pushover curve. With regard to the ABF system, damage states are defined on the final branch of a quadrilinear 'typical' bridge pushover curve, whose third branch initiates with the closure of the longitudinal joint between the deck and the abutment, and the subsequent activation of the ABF system. When the ABF system is not modelled explicitly, approximate damage state definitions are provided.

The final step is the derivation of generalised fragility curves. The probability of exceedance of a given damage state is firstly expressed as a function of the damage parameter, i.e. the bridge deck displacement. Then, the evolution of damage diagram (the primary vulnerability curve) is plotted using the target displacement for increasing earthquake intensity levels expressed by the earthquake parameter (here the peak ground acceleration, A_g), which is then used in combination with the median damage state threshold values of the damage parameter to derive the corresponding median threshold value of A_g. Thus, idealizing the probability density function as lognormal, the probability of

exceedance of a certain damage state can be calculated from the following relationship

$$P_f = \Phi\left[\frac{1}{\beta_{tot}} \cdot \ln\left(\frac{A_{g,m}}{A_{g,DSi,m}}\right)\right] \quad (1)$$

where: P_f is the probability of exceedance of damage state DS_i,
β_{tot} is the total lognormal standard deviation which represents the total uncertainty (herein a value of 0.6 is adopted in line with similar studies [4])
$A_{g,DSi,m}$ is the median threshold value of the peak ground acceleration for damage state DS_i

The corresponding fragility curve is the plot of Eq. (1). Generalised fragility curves are derived repeating the aforementioned procedure for various angles of incidence of the seismic action between 0° and 180°.

3 SOIL-BRIDGE INTERACTION

3.1 Modelling of the abutment-backfill-foundation system

The abutment-backfill-foundation system was modelled by Sextos et al. [12, 14] in 3-dimensional space using the commercial finite element analysis software ABAQUS [1]. The backfill, the embankment, and the foundation soil discretization was made using tetrahedral solid elements, while brick elements were used to model abutments and pile groups. A dense finite element grid was set up for the areas of stress concentration and/or abrupt geometry change, i.e. in the vicinity of the abutment, backfill, and pile groups. Then, pushover analysis was performed individually for the two principal bridge directions leading to the corresponding idealised, bilinear pushover curves (Fig. 1); it has to be noted that this bilinearisation involves a significant degree of subjectiveness. Having obtained the abutment-embankment stiffness for various levels of earthquake intensity, and assuming (for simplicity) that the dynamic and the static stiffness of the particular system do not differ substantially [16] the bilinear curve obtained through nonlinear static analysis was used for defining the hysteresis loop required for dynamic analysis. The damping of the ABF system was also derived according to the literature [16].

3.2 Modelling of pier foundations

Soil-bridge interaction at the pier foundation base [14] was taken into account by considering the pile-to-pile interaction and forming the corresponding 6DOF dynamic impedance matrices with the use of the computer code ASING [13]. For the case of nonlinear static analysis it is only the stiffness matrix that is considered.

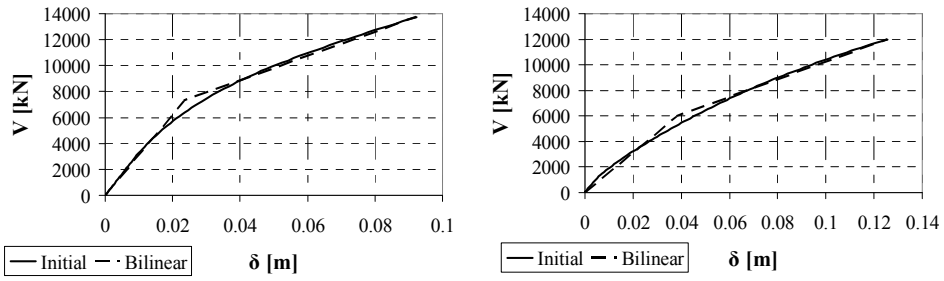

a. Longitudinal direction *b.* Transverse direction

Figure 1. Pushover curves of the abutment-backfill-foundation system [12, 14].

4 APPLICATION TO A STRAIGHT BRIDGE

4.1 Description and modelling of the selected bridge

The selected bridge (Fig. 2) is an overpass crossing the Egnatia Odos motorway in Northern Greece. It is a 3-span bridge of 71.2m total length (19.6 + 32.0 + 19.6) with a continuous deck consisting of an 11m wide prestressed tee-section with two cylindrical voids of 1.10m diameter. The two piers (M1 and M2) are 8.5m high, they have a solid circular section with 1.7m diameter, and are monolithically connected to the deck. The deck movement at the abutments is free up to 0.12m when the longitudinal gap is designed to close and the ABF system is activated. In the transverse direction the deck movement is restrained by stoppers without any gap. The foundation of the bridge consists of 2×2 pile groups with pile lengths of 32m in pier M1 and 28m in pier M2, respectively.

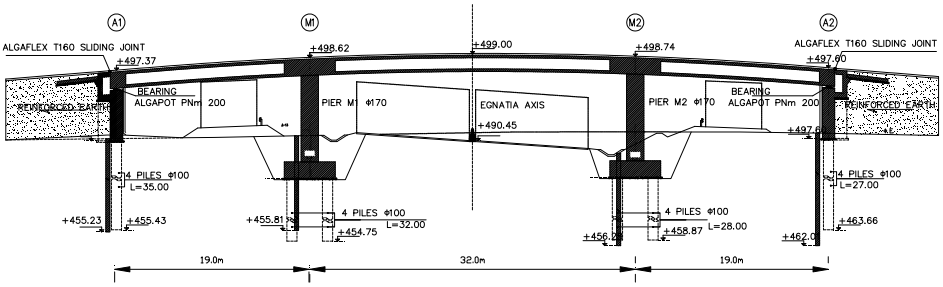

Figure 2. Elevation view of the selected overpass bridge (Pedini bridge)

The bridge is analysed using the SAP2000 finite element software [3]. The deck and the two piers are modelled using frame elements. As explained previously, the ABF system is modelled implicitly in a series system with the 0.12m gap while the 6×6 dynamic impedance matrices at the pier-foundation level are

modelled as 6DOF springs and dashpots ('SBI' case in Table 1). In addition, another bridge model is created where soil-bridge interaction is ignored ('Non-SBI' case). In this model the ABF system is not modelled in the longitudinal direction, while in the transverse direction only its initial (elastic) stiffness is considered, i.e. it is modelled as a linear spring. The modal periods of the two prevailing modes in the longitudinal and transverse directions for both the SBI and the Non-SBI models are summarized in Table 1 together with the corresponding percentage of mass activated in each direction. It is seen that in the longitudinal direction, consideration of foundation compliance (SBI case) results into a 10% increase in the fundamental period because piers dominate the bridge's longitudinal response. In the transverse direction the corresponding increase is only 0.8% because the significant transverse stiffness of the almost fully restrained bridge deck, due to the also significant stiffness of the ABF system (K_{el}=156251.6 kN/m), dominates the bridge response. In contrast, the mass activated in each direction remains practically unaffected.

Table 1. Dynamic characteristics of the bridge considering and ignoring soil-structure interaction

Prevailing Mode	SBI case		Non-SBI case	
	T [sec]	ε [%]	T [sec]	ε [%]
Longitudinal	0.82	99.4	0.73	99.8
Transverse	0.73	91.5	0.72	91.2

4.2 Evaluation against dynamic analysis results

At first, the proposed methodology for the derivation of static pushover curves under arbitrary angle of incidence of the seismic action is evaluated against the more accurate inelastic dynamic analysis. Due to space limitations only the SBI case is evaluated here; the Non-SBI case has already been evaluated in [8]. The seismic action is modelled using the major horizontal component (single-component seismic action) of the Thessaloniki record of the 1978 Volvi earthquake described in Table 2. The selection of a single record is justified on the grounds that the uncertainty due to the seismic action is assumed as part of the total uncertainty which, as described earlier, is set to 0.6 (see §2).

Table 2. Characteristics of selected ground motion

Place	Station	Date	Time	M	R [km]	Components	A_g [g]
Thessaloniki	City Hotel	20/06/78	08:03:21	6.1	29	N-S	0.139
						E-W	0.146

For the evaluation, the 'dynamic pushover curves' using the maximum displacement and the corresponding simultaneous shear force [δ_{max}–$V_b(t_{max})$] are

derived from response-history analysis and are then plotted on the same diagram (Fig. 3) with the corresponding δ_{max}–V_b points derived using the quadrilinear pushover curve for the longitudinal direction and the equal displacement approximation, and the pushover curve itself. From Fig. 3 it is observed that over the entire displacement range, the δ_{max}–$V_b(t_{max})$ points lie closely to the quadrilinear pushover curve, with an exception in the range after yielding of the ABF system where a small difference (10%) is observed. This matching is expected because both the bilinear (Fig. 4a) and the quadrilinear (Fig. 4b) pushover curves prior and subsequent to the activation of the ABF system, respectively, are the envelopes of the corresponding $\delta(t)$-$V_b(t)$ diagrams.

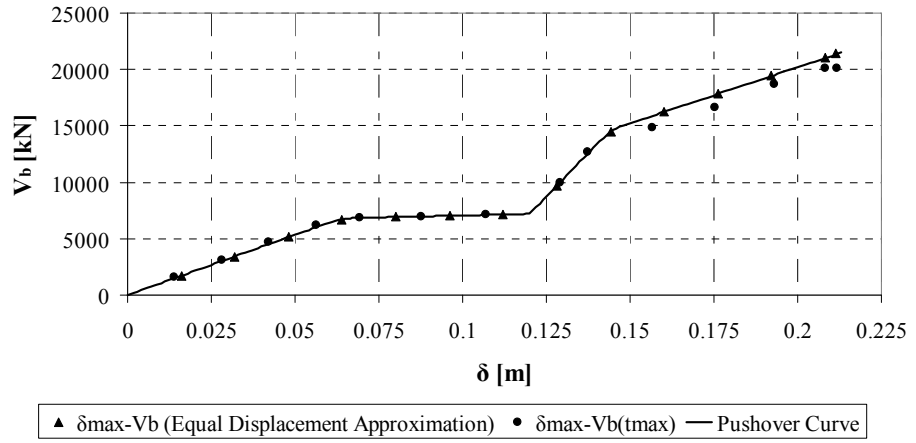

Figure 3. Dynamic and static pushover curves in longitudinal bridge direction – SBI case – Thessaloniki earthquake – Single-component seismic action

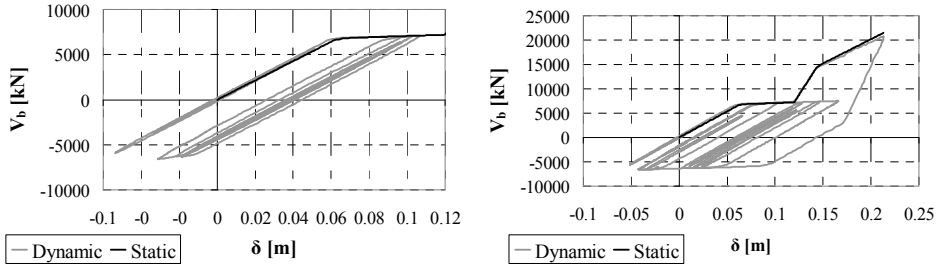

a. Bilinear pushover curves *b.* Quadrilinear pushover curves

Figure 4. $\delta(t)$-$V_b(t)$ diagrams and the corresponding envelope functions (pushover curves)

Comparing the δ_{max}–$V_b(t_{max})$ points with the corresponding δ_{max}–V_b points, it is observed that until the ABF system is activated, the equal displacement rule

leads to 13% larger displacements, mainly because the seismic input energy in dynamic analysis is smaller than the corresponding one in static analysis due to the modelling of radiation damping. After the ABF system is activated, the difference between the equal displacement approximation and the dynamic response is reduced to 5%. Since the aforementioned differences are reasonably small, the use of the equal displacement rule to estimate the target displacement over the whole range of displacements is deemed to be justified.

4.3 Effect of soil-bridge interaction on bridge response and fragility

The proposed methodology for the derivation of bridge pushover curves is applied here for 7 angles of incidence from 0° to 90° (step of 15°). Target displacements are estimated using the equal displacement approximation, which was found (§4.2) to be valid for the entire range of bridge displacements. From the derived pushover curves (Fig. 5) it is observed that starting from the case of longitudinal excitation (α=0°) the shape of pushover curves remains quadrilinear up to the angle of 45°, which implies that bridge response is substantially affected by the activation of the abutment-backfill system. Regarding bridge failure, it is seen that the critical excitation direction is the longitudinal one (α=0°, $A_{g,u}$=1.32g), i.e. where the effect of the activation of the ABF system is maximised. The least critical direction is at an angle of α=60° (A_{gu}=2.27g), i.e. when the response in the transverse direction starts to become dominant; it is important that α=90° is *not* the least critical direction.

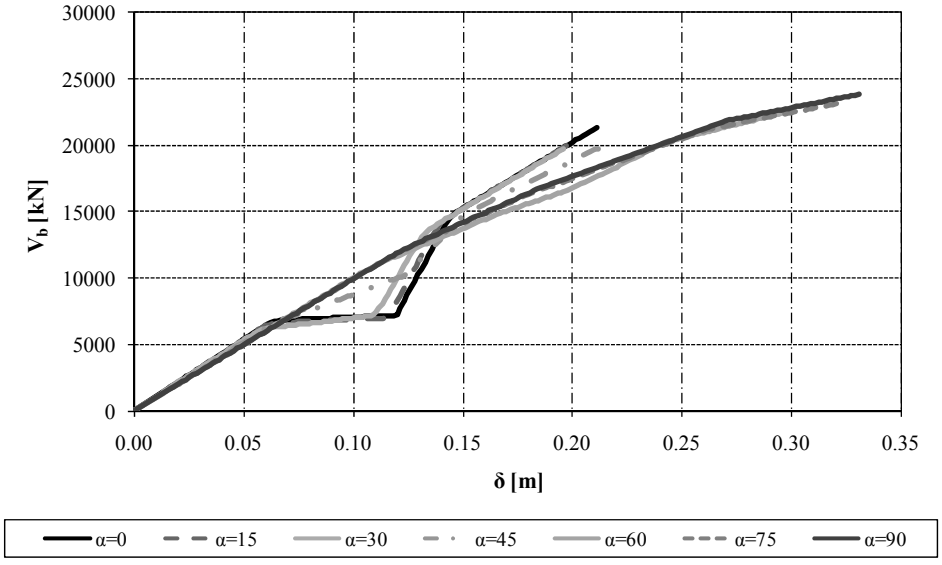

Figure 5. Pushover curves for overpass bridge, for various angles of incidence.

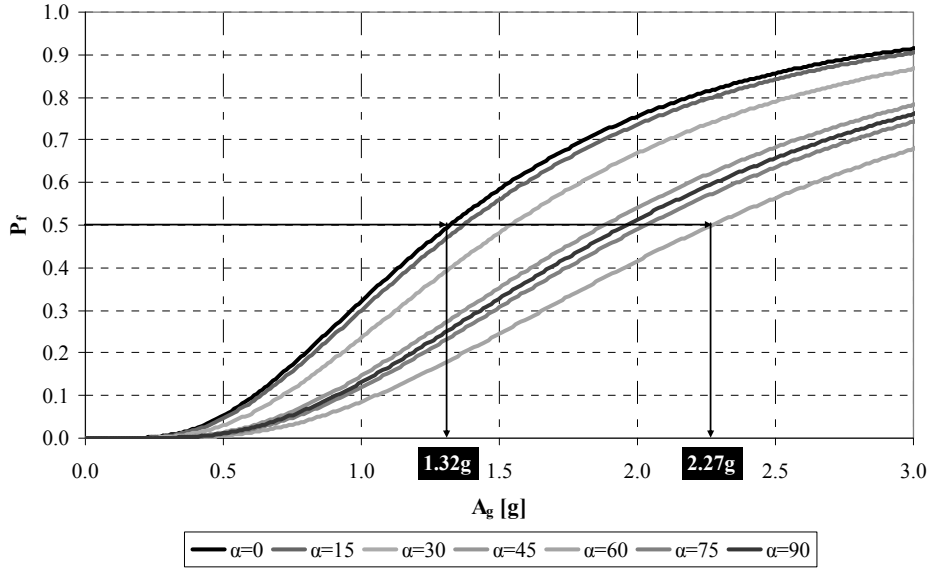

Figure 6. Generalised fragility curves for overpass bridge – DS4: Failure/Collapse - (SBI case)

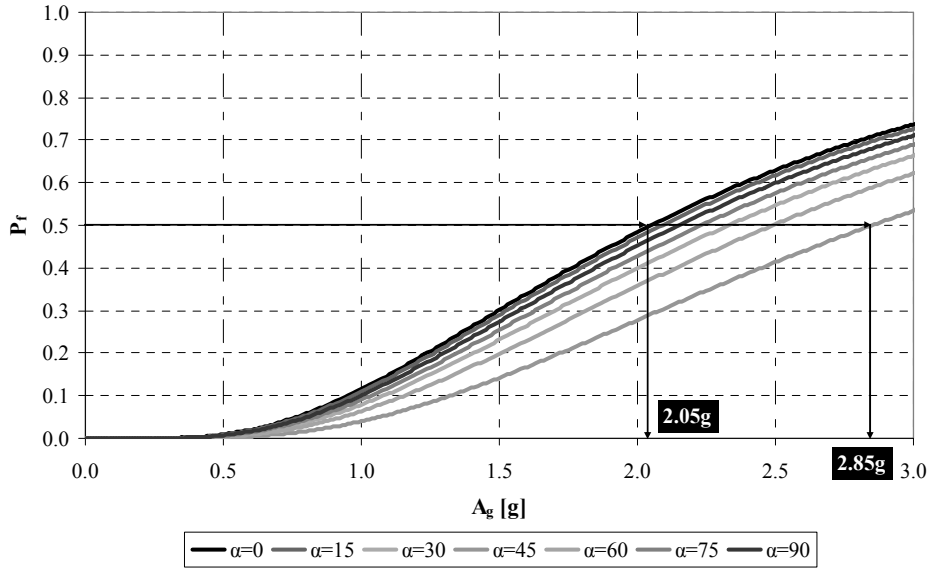

Figure 7. Generalised fragility curves for overpass bridge – DS4: Failure/Collapse - (Non-SBI case)

Generalised fragility curves were derived for the overpass bridge for all damage states described in [8, 9], for both SBI and Non-SBI. The curves derived for the

last damage state (DS4: failure/collapse) for the SBI case are shown in Fig. 6; and those for the Non-SBI case are shown in Fig. 7. At first, it is observed that when soil-structure interaction is accounted for, the most and least critical directions match the ones revealed by the individual pushover analyses (Fig. 5), a fact that is anticipated since the collapse damage state is defined on the basis of the ultimate bridge displacement. Comparing the median threshold values of A_g for the critical and the least critical direction between the SBI and the Non-SBI case, it is also observed that consideration of soil-bridge interaction leads to a significant decrease in the threshold values, from 20% (in the least critical direction, α=60°) to 36 % (in the most critical direction, α=0°).
Finally, in the SBI case, the bridge fragility is found to be significantly affected by the angle of incidence of the seismic action given that the difference in median threshold values of A_g between the critical and the least critical direction is approximately 70%, whereas if soil-bridge interaction is neglected this difference becomes 40%.

5 CONCLUSIONS

In the paper a methodology for the derivation of generalised bridge fragility curves for arbitrary angle of incidence of the seismic action proposed by the authors is extended to include the effect of soil-bridge interaction, and is applied to a straight overpass bridge.
The case-study shows first that soil-bridge interaction results only to a small increase (10%) in the period of vibration in the longitudinal direction while it has negligible effect (0.8%) in the transverse direction. The proposed methodology for the derivation of pushover curves for arbitrary angle of incidence of the seismic action was evaluated against dynamic inelastic analysis and it was found that both the bilinear and the quadrilinear forms of pushover curves envelope the corresponding dynamic response (dynamic pushover curves) and that the equal displacement approximation is a valid assumption, also in the case where the soil-bridge interaction is taken into account, at least for the specific case studied.
From the derived pushover and generalised fragility curves for arbitrary angle of incidence of the seismic action, it is also found that the activation of the abutment-backfill-foundation system dominates the bridge response up to an angle of incidence of 45°. Regarding bridge failure, referring either to its seismic response or its fragility, the critical direction is the longitudinal one while the least critical is found to be for a 60° angle, i.e. not a principal direction. It was also interesting to observe that consideration of soil-bridge interaction increases the predicted fragility of the bridge (lower damage thresholds, up to 36%) as well as the effect of varying angle of incidence (70% difference between critical and least critical direction, compared to 40% in the case that interaction is neglected).

REFERENCES

[1] ABAQUS/PRE, *User's Manual*, Hibbit, Karlsson and Sorensen Inc., 2004.

[2] Arias A, "A measure of earthquake intensity". In: Hansen RJ, editor. Seismic Design for Nuclear Power Plants. M.I.T. Press: Cambridge, Massachusetts, pp. 438-483, 1970.

[3] CSI, *CSI Analysis Reference Manual for SAP2000®, ETABS®, and SAFE®*, Computers & Structures Inc., Berkeley, California, 2009.

[4] FEMA-NIBS, *Multi-Hazard Loss Estimation Methodology - HAZUS-MH MR4: Earthquake Model Technical Manual*, Federal Emergency Management Agency (under a contract with the National Institute of Building Sciences), Washington, D.C., 2003.

[5] Kappos, AJ, Manolis, GD, Moschonas, IF, "Seismic assessment and design of R/C bridges with irregular configuration, including SSI effects", Engineering Structures, Vol. 24, No. 10, pp. 1337-1348, 2002.

[6] Kappos, AJ, Potikas, P, Sextos, AG, "Seismic assessment of an overpass bridge accounting for non-linear material and soil response and varying boundary conditions", *CD-ROM Proc. ECCOMAS Thematic Conference on Computational Methods in Structural Dynamics and Earthquake Engineering - COMPDYN 2007*, Paper No. 1580, Rethymno, 2007.

[7] Kappos, AJ, Sextos, AG, "Effect of foundation type and compliance on seismic response of RC bridges", Journal of Bridge Engineering, ASCE, Vol. 6, No. 2, pp.120-130, 2001.

[8] Moschonas, IF, Kappos, AJ, "Generalised fragility curves for bridges, for arbitrary angle of incidence", *CD-ROM Proc. ECCOMAS Thematic Conference on Computational Methods in Structural Dynamics and Earthquake Engineering - COMPDYN 2009*, Paper No. 186, Rhodes, 2009.

[9] Moschonas, IF, Kappos, AJ, "Generalised fragility curves for bearing-supported skew bridges, for arbitrary angle of incidence of the seismic action", *CD-ROM Proc. ECCOMAS Thematic Conference on Computational Methods in Structural Dynamics and Earthquake Engineering - COMPDYN 2011*, Paper No. 377, Corfu, 2011.

[10] Moschonas, IF, Kappos, AJ, Panetsos, P, Papadopoulos, V, Makarios, T, Thanopoulos, P, "Seismic fragility curves for greek bridges: methodology and case studies", Bulletin of Earthquake Engineering, Vol. 7, No. 2, pp. 439-468, 2009.

[11] Penzien, J, Watabe, M, "Characteristics of 3-dimensional earthquake ground motions.", Earthquake Engineering & Structural Dynamics, Vol. 3, No. 4, pp. 365-373, 1974.

[12] Sextos, AG, Mackie, KR, Stojadinović, B, Taskari, O, "Simplified P-y Relationships for modelling embankment-abutment Systems of Typical California Bridges", *CD-ROM Proc. 14th World Conference on Earthquake Engineering*, Paper No. 05-02-0032, Beijing, 2008.

[13] Sextos, AG, Pitilakis, KD, Kappos, AJ, "Inelastic dynamic analysis of RC bridges accounting for spatial variability of ground motion, site effects and soil-structure interaction phenomena. Part 1: Methodology and analytical tools", Earthquake Engineering & Structural Dynamics, Vol. 32, No. 4, pp. 607-627, 2003.

[14] Sextos, AG, Taskari, O, "Comparative Assessment of Advanced Computational Tools for Embankment-Abutment-Bridge Superstructure Interaction", *CD-ROM Proc. 14th World Conference on Earthquake Engineering*, Paper No. 05-02-0031, Beijing, 2008.

[15] Taskari, ON, Sextos, AG, Kappos, AJ "3D Finite Element Modelling of a Highway Bridge Considering the Effect of Soil and Foundation", *CD-ROM Proc. 6th GRACM International Congress on Computational Mechanics*, Thessaloniki, 2008.

[16] Zhang, J, Makris, N, "Kinematic response functions and dynamic stiffnesses of bridge embankments", Earthquake Engineering & Structural Dynamics, Vol. 31, No. 11, pp. 1933-1966, 2002.